

Femtosecond Carrier Thermalization in Dense Fermi Seas

W. H. Knox, D. S. Chemla, G. Livescu, J. E. Cunningham, and J. E. Henry

AT&T Bell Laboratories, Holmdel, New Jersey 07733

(Received 31 May 1988)

We study the effects of excess thermalized electron and hole populations on femtosecond carrier thermalization in optically excited GaAs quantum wells. In modulation-doped samples we find that the presence of $3 \times 10^{11} \text{ cm}^{-2}$ electrons produces an extraordinarily fast carrier thermalization (faster than 10 fs); however, the presence of the same density of holes yields a thermalization time close to that of undoped samples (≈ 60 fs). These results give the first direct evidence that electron-electron interactions yield the dominant contributions to carrier thermalization in GaAs and also show that the electron distribution function itself influences thermalization dynamics.

PACS numbers: 78.50.Ge, 71.45.-d, 72.15.Lh, 78.47.+p

Ultrashort optical excitation now allows us to establish nonthermal (i.e., non-Fermi) distributions of electrons and holes in the conduction and valence bands of semiconductors and to observe them in such a short time that they have not yet scattered out of the states into which they were injected. The carriers can then thermalize (i.e., assume Fermi-type distributions) within their respective energy bands by a variety of scattering processes, including carrier-carrier scattering (CCS), phonon and plasmon emission, intervalley scattering, etc.¹ With excitation high above the band edge, all of these processes are active and they contribute to thermalization on the femtosecond time scale. Several experiments have been done in this regime with GaAs and excitation at 625 nm.^{2,3}

It is possible to isolate CCS from the other relaxation processes by near-band-gap excitation. In this case, the only allowable thermalization mechanism is CCS since essentially the entire carrier distribution function is below the threshold for the competing processes and transitions from the spin-orbit split-off band are avoided. This condition has been achieved in GaAs bulk⁴ and quantum well structures (QWS).⁵

When a photon is absorbed by a semiconductor, for every electron which is created, one hole is created. Therefore, even in the simplified condition of near-band-gap excitation where only CCS is operative, the interaction has three terms: electron-electron ($e-e$), electron-hole ($e-h$), and hole-hole ($h-h$) scattering. Because the electrons and holes have different properties such as mass, phonon interaction, etc., these three scattering mechanisms are expected to be different in nature. Furthermore, the carrier distribution in k space should alter the dynamics. In the present work we investigate experimentally these scattering mechanisms and the influence of an e or h distribution near $k=0$ on the femtosecond carrier thermalization process in GaAs QWS. We accomplish this by monitoring the occupation of specific energy states using femtosecond time-resolved optical-absorption measurements. We perform first a set

of experiments in undoped GaAs QWS at small excess energy (≈ 20 meV), then repeat the experiments in doped quantum wells. We use a technique known as modulation doping⁶ in which carrier scattering is isolated from impurity scattering by doping of the barriers only. When the barriers are doped with Si (Be), excess electrons (holes) spill into the well and create a dense Fermi sea of electrons (holes) which are in thermal equilibrium with the lattice which is at room temperature for the present experiments. Since our experimental technique is sensitive to the *energy distribution* of the carriers, we directly measure the *inelastic-scattering* contribution to CCS. In each case we determine the carrier thermalization time by comparison of the data with a relaxation-time approximation model, which we describe briefly after discussion of the experiments.

The experimental technique is as follows. Laser pulses of 100-fs duration at a wavelength of 805 nm are generated and amplified at 8-kHz repetition rate with a copper-vapor laser-pumped amplifier.⁷ These pulses, when focused into a 1-mm jet of ethylene glycol, produce white-light continuum pulses, with the center wavelength at 805 nm, yielding continuum intensities which are several orders of magnitude larger than previously available.⁵ A small portion of this infrared continuum (4%) is split off and passed through a variable time-delay stage and focused to a 15–20- μm -diam spot in the sample, and the transmitted probe light is detected by a spectrometer and Reticon optical multichannel analyzer. The rest of the continuum pulse is passed through an interference filter to select a 100-fs pump pulse of the desired spectrum and focused to a 50–60- μm -diam spot overlapping the probe pulse on the sample. The cross-correlation measurement between the selected pump and probe pulses is 150 fs full-width at half-maximum, corresponding to 100-fs selected pump pulse and 100-fs probe pulse widths. We directly measure the differential absorption spectrum by inserting a shutter into the pump beam and chopping it at a 6-Hz rate while synchronously detecting the change in the transmitted probe spectrum.

This process is repeated 200 times at each time delay for the data shown here.

In QWS, long-range direct screening does not influence significantly the absorption of the correlated electron-hole systems⁸⁻¹⁰ (excitons and Fermi-edge singularities^{11,12}) which is essentially governed by the occupation of the lowest available states close to $k \approx 0$.⁸⁻¹¹ Therefore, the evolution of the absorption *at the injection* energy yields information on the time it takes the carriers to scatter out of the state in which they were generated, whereas the evolution *at the absorption edge* gives information on the time it takes them to reach the extrema of their respective bands. In a previous experiment,⁵ undoped 9.6-nm-thick GaAs quantum wells were excited optically with 100-fs pulses near the band edge at a photocarrier density of $N_{e,h}^{ph} \approx 2 \times 10^{10} \text{ cm}^{-2}$. Spectral hole burning was observed in a region around the pump spectrum, and the carriers were observed to thermalize in about 100 fs. With the much higher excitation energy now available, we have investigated the density dependence of the thermalization process in the same sample.⁵ Figure 1(a) shows a set of differential transmission spectra, $\Delta T/T_0$, at 66-fs intervals for a photocarrier density $N_{e,h}^{ph} \approx 5 \times 10^{11} \text{ cm}^{-2}$.¹³ In an energy region centered about the pump spectrum, a broad hole burning is observed followed by a rapid thermalization to a Boltzmann-type distribution. We also see that at $\Delta t = 0$, the bleaching in the region of the exciton resonances ($\hbar\omega \approx 1.46 \text{ eV}$) has already reached its final value, in contrast with the low-density excitation⁵ wherein at $\Delta t = 0$ the exciton bleaching is only $\frac{1}{6}$ of its final value which is obtained at much longer times ($\Delta t > 200 \text{ fs}$). Experiments performed at various excitation densities confirm this trend, demonstrating that excitons bleach faster as the density is increased. This occurs because as the density increases, CCS ejects carriers out of their initial states faster and they reach the bottom of the band earlier. By comparison with our relaxation-time approximation model, we find that τ_{th} reduces from ≈ 100 to 30 fs when the photocarrier density goes from $N_{e,h}^{ph} \approx 2 \times 10^{10} \text{ cm}^{-2}$ to $5 \times 10^{11} \text{ cm}^{-2}$. The weak dependence of the thermalization time with density, scaling approximately as $\tau_{th} \propto (N_{e,h}^{ph})^{-1/4}$, originates from the near cancellation of two competing processes.¹⁴ Thermalization by CCS requires numerous scattering events during which significant energy is exchanged. At low excitation densities, the intrinsic scattering rate is high, but elastic scattering dominates, exchanging small amounts of energy per collision, thus resulting in a relatively long thermalization time (100 fs). At high densities, the intrinsic scattering rate is reduced by screening and degeneracy, but the probability for inelastic scattering, which exchanges much more energy per collision, increases significantly; hence the thermalization speeds up only moderately¹⁴ (30 fs). It is interesting to note that the thermalization time that we

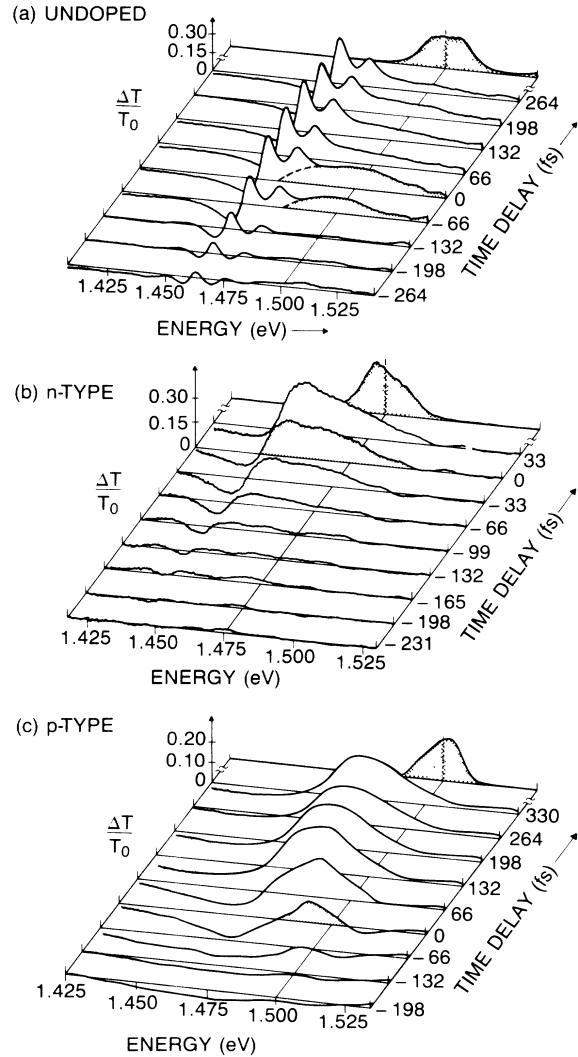


FIG. 1. Differential absorption spectra for (a) the undoped QWS at 66-fs time-delay intervals; (b) the *n*-modulation doped QWS at 33-fs time-delay intervals; and (c) the *p*-modulation doped QWS at 66-fs time-delay intervals.

measure at the highest density is significantly larger than the time constant obtained by Lin *et al.*³ in bulk GaAs for comparable densities. This difference is due to the fact that in our experiment CCS is the only relaxation mechanism involved in the thermalization. Nonetheless, the weak dependence which we find for the density dependence of the CCS rate in our high-density experiments is consistent with the weak dependence which has been found in other experiments.²

The *n*-type sample consists of 12-nm wells and 40-nm barriers, the central 10 nm of which were doped with Si. This provided an areal electron density of about $N_e^{dop} \approx 3 \times 10^{11} \text{ cm}^{-2}$ in the wells, as determined by Hall measurements and a room-temperature mobility $\mu = 2000 \text{ cm}^2/\text{V s}$. In modulation-doped QWS, the lowest

states accessible by optical absorption are "Fermi-edge singularities"^{11,12} which appear at the Fermi energy. Figure 1(b) shows the differential transmission spectra at 33-fs intervals for a density of photocarriers $N_{e,h}^{ph} \approx 3 \times 10^{11} \text{ cm}^{-2}$ and excess energy above the Fermi edge as for the undoped case just discussed. No evidence of a nonthermal distribution is observed. The differential spectra now rise as a uniform Boltzmann-type distribution for all times; quite a different result than in the undoped case. It is our contention that in this case, carrier thermalization is so rapid that it occurs on a time scale below the system time resolution. Our relaxation-time approximation model indicates that $\tau_{th} < 10 \text{ fs}$ is required to reproduce this result. The spectra show instantaneously a small negative dip at the low-energy edge which indicates a slight decrease of the transmission. It originates from a slight shift and broadening at the Fermi edge as the photocarriers are injected. This experiment shows that thermalization is much faster in the presence of a thermalized Fermi sea of electrons.

The *p*-type sample consists of 11-nm wells with 40-nm barriers, the central 10 nm of which were doped with Be, yielding an areal hole density in the well of $N_h^{dop} \approx 2 \times 10^{11} \text{ cm}^{-2}$ and a room-temperature mobility $\mu = 200 \text{ cm}^2/\text{V s}$. Figure 1(c) shows the differential transmission spectra under identical conditions as for the *n*-type cases but at 66-fs intervals. A clear spectral hole burning is again observed around delay time $\Delta t = 0$ in a region of energy around the pump spectrum. A thermalized profile is reached in about 100 fs, but at early times the line shape is much more complicated than in the two previous cases. The relatively complex differential spectrum at $\Delta t = 0$ has a simple interpretation. In Fig. 2 we show the absorption spectra at $\Delta t = -200, 0,$ and $+400 \text{ fs}$ together with the differential absorption at $\Delta t = 0$ and the pump-pulse spectrum. The large negative dip in the differential absorption spectrum is caused by an instantaneous broadening and shift of the Fermi edge which is apparently larger than in the case of the *n*-type sample. The origin of such a strong reaction of the Fermi sea of holes is not understood at present, but it could be related both to the complex valence-band structures of QWS and to the dependence of many-body effects upon the mass of the carriers in the Fermi sea. Then, as the photocarriers thermalize, they fill up the bands and the absorption edge shifts to higher energy. We note that the hole-burning signal appears at a slightly lower energy than the pump energy. This seems to be a reproducible feature and may be the result of renormalization effects. In our previous experiment at low densities in undoped quantum wells,⁵ the hole was also burned at a slightly lower energy; however, at high densities, the hole burning is symmetric about the pump as a result of saturation [Fig. 1(a)].

We find by comparison to our model that in the *p*-type case the thermalization time is about 60 fs. This result

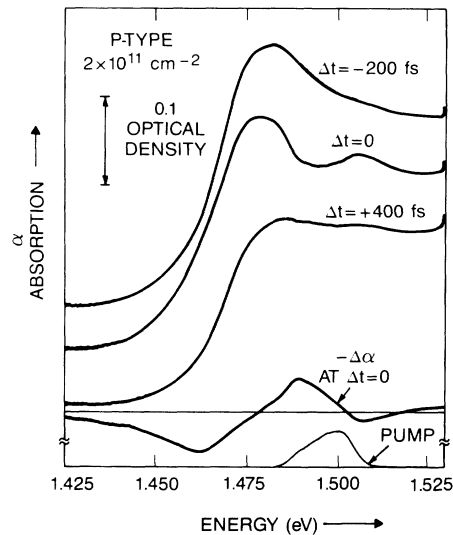


FIG. 2. Absorption spectra of *p*-modulation doped sample at time delays $\Delta t = -200, 0,$ and $+400 \text{ fs}$, and differential absorption spectrum at $\Delta t = 0$ with pump spectrum. Note the small shift between the hole burning and the pump-pulse spectrum, and the shift of the absorption edge due to band filling between $\Delta t = 0$ and $\Delta t = +400 \text{ fs}$.

stands in marked contrast with the *n*-type case where we found a thermalization time of less than 10 fs, but resembles more closely the case of the intrinsic sample. Thus, apparently the excess hole population at the top of the valence band is less effective in thermalizing the photocarrier distribution than an excess electron population of about the same density at the bottom of the conduction band. Our interpretation of this result is that because of the large mass difference between *e* and *h*, *e-h* scattering is mostly elastic and thus does not yield fast thermalization. It is worth noting that by use of luminescence techniques, momentum-relaxation times $\approx 80 \text{ fs}$ were measured¹⁵ for electrons in quantum wells *p*-modulation doped at $N_h^{dop} \approx 1.6 \times 10^{11} \text{ cm}^{-2}$.

The effects of femtosecond optical injection of carriers in dense two-dimensional *e-h* systems is a complicated problem in many-body physics that has not been solved to date. Even modeling correctly the thermalization in our simple case with only CCS in the Γ valley is extremely complicated. One approach to this problem which has recently been developed makes use of heavy numerical ensemble Monte Carlo simulations.¹⁴ Although we have succeeded in observing nonthermal distributions in QWS over a wide range of parameters, we need a model of the relaxation to deduce time constants for thermalization. In order to interpret our data in simple terms, we have developed a model that summarizes the time evolution of the carrier distribution in a single parameter, the thermalization time τ_{th} , and yet incorporates the major ingredients of the experiment. We as-

sume that on the time scale of the observation, no energy is exchanged with the lattice and there is no loss of carriers due to intervalley scattering or recombination. We assume a local equilibrium relaxation toward the Fermi distribution corresponding to the instantaneous number of carriers present in the sample. We account for absorption saturation in the 2D continuum. The time dependence of the driving term is assumed to be a 150-fs FWHM hyperbolic secant pulse, in agreement with the measured cross-correlation function. We find that this simple model gives a description of the dynamics of the population in excellent agreement with that of the Monte Carlo simulations¹⁴ in terms of both its time evolution and energy distribution. The τ_{th} quoted in the previous sections were obtained by simultaneous comparison of the experimental time evolution at the lowest energy level and at the injection energy with the model. In particular, we find that when τ_{th} becomes small compared to the time width of the driving function, the nonthermal distribution around the driving-term spectrum becomes less pronounced. For $\tau_{th} < 10$ fs, nonthermal distributions are not resolved.

In conclusion, we have directly demonstrated that the thermalization rate is greatly increased by the addition of a dense thermalized Fermi sea of electrons, but it is not increased by the addition of a dense thermalized Fermi sea of holes. In the undoped case, even at high excitation densities ($5 \times 10^{11} \text{ cm}^{-2}$), we resolve nonthermal distributions with about 30-fs thermalization times; however, the addition of a less-dense thermalized Fermi sea of electrons produces faster thermalization. This shows clearly that the electron occupation function as well as the total electron density is important in determining the thermalization dynamics. In particular, these results imply that occupation at $k=0$ increases the thermalization rate. In the undoped case, there is no occupation at $k=0$ at time $t=0$, and so the thermalization rate is initially small and may be dynamically modified by the changing occupation. We have also evaluated the relaxation approximation solutions for this case, using a thermalization rate consisting of a constant term plus a term proportional to the occupation at $k=0$. This approach, albeit a heuristic one, yields results which are consistent with the experiments, but more work is needed

on this point. Figure 1 strikingly evidences the qualitatively different thermalization behaviors of the undoped, n -doped, and p -doped samples.

We wish to thank S. Schmitt-Rink, D. A. B. Miller, J. Shah, and S. M. Goodnick for many stimulating discussions.

¹J. Shah, IEEE J. Quantum Electron. **22**, 1728 (1985).

²C. L. Tang and D. J. Erskine, Phys. Rev. Lett. **51**, 840 (1983).

³W. Z. Lin, J. G. Fujimoto, E. P. Ippen, and R. A. Logan, Appl. Phys. Lett. **50**, 124 (1987).

⁴J. L. Oudar, D. Hulin, A. Migus, A. Antonetti, and F. Alexandre, Phys. Rev. Lett. **55**, 2074 (1985).

⁵W. H. Knox, C. Hirlimann, D. A. B. Miller, J. Shah, D. S. Chemla, and C. V. Shank, Phys. Rev. Lett. **56**, 1191 (1986).

⁶R. C. Dingle, H. Stormer, A. C. Gossard, and W. Wiegmann, Appl. Phys. Lett. **33**, 665 (1978); A. C. Gossard and A. Pinczuk, in *Synthetic Modulated Structures*, edited by L. L. Chang and B. C. Giessen, Materials Sciences Series (Academic, New York, 1985).

⁷W. H. Knox, J. Opt. Soc. Am. B **4**, 1771 (1987).

⁸S. Schmitt-Rink, D. S. Chemla, and D. A. B. Miller, Phys. Rev. B **32**, 6601 (1985).

⁹D. S. Chemla, S. Schmitt-Rink, and D. A. B. Miller, in *Optical Nonlinearities and Instabilities in Semiconductors*, edited by H. Haug (Academic, New York, 1988).

¹⁰D. S. Chemla, I. Bar-Joseph, J. M. Kuo, T. Y. Chang, C. Klingshirn, G. Livescu, and D. A. B. Miller, IEEE J. Quantum Electron. (special issue on quantum wells and superlattices) (to be published).

¹¹A. E. Ruckenstein and S. Schmitt-Rink, Phys. Rev. B **35**, 7551 (1987).

¹²G. Livescu, D. A. B. Miller, D. S. Chemla, M. Ramaswamy, T. Y. Chang, N. Sauer, A. C. Gossard, and J. H. English, IEEE J. Quantum Electron. (special issue on quantum wells and superlattices) (to be published).

¹³We estimate the carrier density by integrating the differential spectrum in the continuum and comparing the bleached area with the two-dimensional density of states.

¹⁴S. M. Goodnick and P. Lugli, Appl. Phys. Lett. **51**, 584 (1987), and in Proceedings of the Hot Electron Conference, Boston, Massachusetts, 1987 (to be published), and Phys. Rev. B **37**, 2578 (1988), and private communication.

¹⁵R. A. Hopfel, J. Shah, P. A. Wolff, and A. C. Gossard, Phys. Rev. Lett. **56**, 2736 (1986), and to be published.

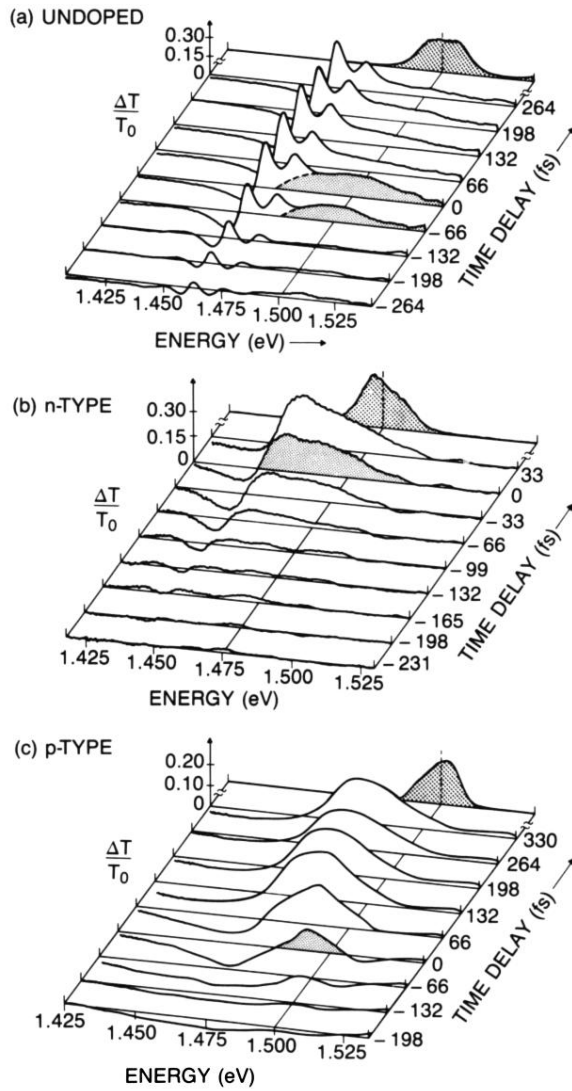


FIG. 1. Differential absorption spectra for (a) the undoped QWS at 66-fs time-delay intervals; (b) the *n*-modulation doped QWS at 33-fs time-delay intervals; and (c) the *p*-modulation doped QWS at 66-fs time-delay intervals.